Continental Shelf Research 187 (2019) 103960

Contents lists available at ScienceDirect

Continental Shelf Research

journal homepage: www.elsevier.com/locate/csr

Revisiting the problem of sediment motion threshold

Yang Yang[a,b], Shu Gao[a,*], Ya Ping Wang[a,c], Jianjun Jia[a], Jilian Xiong[c], Liang Zhou[a]

[a] *State Key Laboratory for Estuarine and Coastal Research, East China Normal University, Shanghai, 200062, China*
[b] *Natural Resources Canada, Geological Survey of Canada (Atlantic), Bedford Institute of Oceanography, Dartmouth, NS, B2Y 4A2, Canada*
[c] *Ministry of Education Key Laboratory for Coast and Island Development, Nanjing University, Nanjing, 210093, China*

ARTICLE INFO

Keywords:
Sediment threshold
Shields curves
Critical shear stress
Turbulence structures
Scale effects
Continental shelf environments

ABSTRACT

The definition of the threshold of sediment motion is critical for continental shelf sediment dynamics. The work by A. Shields laid the foundation for this research direction, leading to the well-known Shields curve. Here we review the most widely used threshold curves that have followed from the original Shields curve over the last 80 years, and propose that in terms of physical processes the threshold (critical Shields parameter) is a function of at least six variables, i.e. grain Reynolds number, grain size distribution, sphericity, roundness, particle cohesiveness and the scale effects of turbulence. Identifying these key factors, we paid a special attention to the role of the scale effects of turbulence. Turbulence was thought to be a random process, but the improvement of measurement techniques revealed that it has both temporal and spatial structures: the magnitude of instantaneous velocity fluctuations varies in time and in location, which can cause the deviation between *in situ* measurements and flume experiments. In coastal and shelf waters, *in situ* measurements of tidal currents and suspended sediment concentrations have revealed that resuspension takes place even though the bed shear stress is well below the Shields curve. Further process and mechanism studies are required to improve the theoretical framework regarding the turbulence structures and their interplay with sediment threshold. The scientific problems for future studies include the establishment of laboratory experiments, *in situ* measurements and process-based modelling under different water depths and hydrodynamic conditions to quantify the scale effects of turbulence; the development of new observation techniques for higher resolution and for extreme environments; development of new data processing methods, including big data methods to analyse turbulence structures; and the quantification of the effects of biological contributions and non-particle components on the family of Shields curves.

1. Introduction

Sediment erosion, transport and redistribution shape the Earth's surface, and are key components of the functioning of the Earth system. In particular, the definition of the threshold of sediment motion is the essential issue in sediment transport theory and practice, owing to its use in many sedimentological, engineering and ecological applications. This topic has attracted global research attention, and has been investigated through laboratory experiments and field observations (e.g. Shields, 1936; Yang, 1973; Miller et al., 1977; Buffington and Montgomery, 1997; Andersen et al., 2007; Shi et al., 2015; Dorrell et al., 2018). In general, the concept of critical shear stress was widely applied to describe the threshold of sediment motion, which is dependent on the balance between hydrodynamic forces acting on a particle and stabilizing forces due to gravity and inter-particles interaction. In other studies, a threshold criterion based on momentum balance was developed to determine threshold conditions (Coleman, 1967; Graf, 1984; Ling, 1995). Nevertheless, the natural environment is complex and highly variable in terms of its prevailing hydrodynamics and sediment dynamics, and the threshold of sediment motion is controlled by the site-specific interactions of physical, geochemical and biological factors.

Due to the difficulty in defining the threshold conditions in the field, a number of empirical threshold curves have been formulated (e.g. Hjulström, 1935; Shields, 1936; Inman, 1949; Miller et al., 1977; Soulsby, 1997; Cao et al., 2006). The doctoral dissertation of Shields (1936) laid the foundation for this research direction, leading to the famous Shields curve that still holds today. The Shields curve represents the relationship between the Shields parameter and the grain Reynolds number, which expresses implicitly the threshold conditions for spherical particles with the same diameter. However, in the natural environment, sediments have different grain size distributions, with

* Corresponding author.
E-mail address: sgao@sklec.ecnu.edu.cn (S. Gao).

https://doi.org/10.1016/j.csr.2019.103960
Received 6 October 2017; Received in revised form 20 July 2019; Accepted 18 August 2019
Available online 26 August 2019

different shapes (i.e., sphericity and roundness). Thus, flume experiments were carried out to include these factors. Using grain size parameters and shape factor values (representing both sphericity and roundness effects), the original Shields curve was expanded to a family of Shields curves (Mantz, 1977; Buffington and Montgomery, 1997; Paphitis et al., 2001, 2002). This was thought to be still insufficient, because the phenomenon of cohesiveness associated with fine-grained sediments was not considered. Subsequently, efforts have been made to distinguish cohesive and non-cohesive sediments. It has been attempted to incorporate the experimental results of the threshold of cohesive sediments into a Shields-type curve (Miller et al., 1977; Dyer, 1986; Righetti and Lucarelli, 2007; Mehta, 2013). Some investigators have linked the threshold to the settling velocity of particles, but the problem of settling velocity itself does not appear to be simpler than the threshold of motion (Komar and Clemens, 1986; Roux, 1998; Paphitis et al., 2002).

Thus far, the threshold of motion (critical Shields parameter) has been analyzed as a function of five variables (i.e., grain Reynolds number, grain size distribution, sphericity, roundness, cohesiveness). Recently, field measurements in some coastal environments have revealed that resuspension may occur even though the bed shear stress is well below the critical value predicted by the Shields curve, suggesting that the scale effects of turbulence also affect the threshold (Yang et al., 2016a; Xiong et al., 2017; Salim et al., 2017, 2018). Turbulence used to be considered as a random process, but the experimental evidence (e.g. Grass, 1971; Willmarth and Lu, 1972) has shown that turbulence has coherent structures, which are generated intermittently by a sequence of powerful and well-organized events within the bottom boundary layer. Sediment resuspension is largely controlled by near-bed turbulence (Dyer, 1986; Zanke, 2003; Yuan et al., 2009; Dey et al., 2011; Ali and Dey, 2016). Although many studies have examined turbulent structures in highly variable marine environments, the precise role of turbulence structures on sediment threshold is yet to be fully understood. It leads to two key questions as to how to quantify the scale effects of turbulence, and how to establish a family of Shields curves at different scale effects of turbulence. Furthermore, uncertainty exists in the field observations (Heathershaw and Thorne, 1985; Chanson et al., 2008; Yang et al., 2016b), and thus a full deployment with high-precision and high-resolution instruments under different flow conditions should be undertaken to reveal the microstructure of turbulence and the interaction between the particles and the fluid. In addition to the factors considered in the Shields curves, the influence of other factors (e.g. biological impacts and non-particle components within the sediment) on sediment threshold may also be important (Grabowski et al., 2011; Malarkey et al., 2015). It is necessary to assess the impact of these factors on the Shields curve.

The purpose of the present contribution is to provide an overview of the most widely used threshold curves that have built on the original Shields curve. The knowledge obtained over the last 80 years from the improvement of the Shields curve is synthesized and the most important factors in relation to the threshold are summarized. On such a basis, special attention is paid to the role of the scale effects of turbulence on sediment threshold. Finally, some critical issues for future investigations are proposed.

2. Efforts made at the time of A. Shields

There are many threshold curves available, but only the most relevant ones, in the context of this paper, will be discussed. Hjulström (1935, 1939) carried out his research in relation to the threshold of sediment motion and developed the Hjulström curve (Fig. 1), which was applied widely due to its simplicity. It shows the relation between the grain diameter and the average flow velocity for erosion, transport and deposition at a water depth of 1.0 m. A minimum value of critical flow velocity is found at a particle size of around 0.5 mm. For large particles, the critical flow velocity increases with an increasing grain diameter, but for small particles, the critical flow velocity increases with a decreasing grain diameter. This opposite trend is explained as a cohesive effect for very small particles (Miedema, 2013). A mathematical description of the Hjulström curve was given by Zanke (1982), and can be well approximated by the following two empirical equations as derived by Miedema (2010):

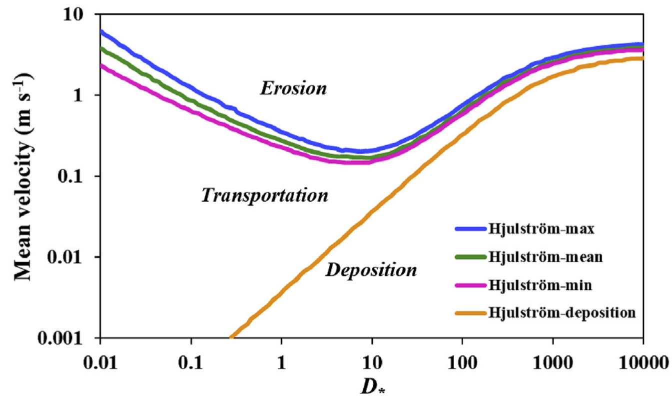

Fig. 1. The modified Hjulström curve, where D_* is the dimensionless grain size (adopted from Miedema, 2013).

$$U_c = 1.5\left(\frac{\upsilon}{d}\right)^{0.80} + 0.85\left(\frac{\upsilon}{d}\right)^{0.35} + 9.5\frac{R_d gd}{1 + 2.25R_d gd} \tag{1}$$

$$U_d = 77\frac{d}{1 + 24d} \tag{2}$$

where U_c and U_d are the critical shear erosion and deposition velocity based on Hjulström curve, respectively, ν is the kinematic viscosity of the fluid, d is the grain diameter, R_d is the relative submerged specific density and g is the acceleration due to gravity.

Similar curves were formulated subsequently by Inman (1949), Lane (1955) and Sundborg (1956), which related the critical shear stress or the flow velocity at a height of 1 m above the seabed (u_{100}) to grain diameter. However, such threshold curves do not include all of the parameters necessary to describe the threshold of sediment motion (Paphitis, 2001). For example, in the definition of threshold by Hjulström (1935), water depth was not included. If water depth is large, the current velocity in the upper part is not relevant to the threshold; if water depth is small, the near-bed shear stress may be large even if the current is weak. Observations from the Jiangsu coast waters, China have revealed such an effect (Gao, 2010). Actually, it is near-bed shear stress, rather than the current velocity, that is most relevant.

Different definitions for the threshold of sediment motion were used (Buffington and Montgomery, 1997). Some investigators used visual observations of grain movement to determine the threshold (Kramer, 1935; Neill and Yalin, 1969; Dancey et al., 2002). The threshold condition in the classic work of Shields (1936) was established by an extrapolation method, in which transport rates were extrapolated to zero, or a low reference value level (Paintal, 1971; Parker and Klingeman, 1982; Beheshti and Ataie-Ashtiani, 2008). Later study suggests that Shields may have used both reference transport rate and visual definitions when combining his data and previous experimental results (Buffington, 1999).

Shields' (1936) flume studies investigated carefully the threshold conditions of particles under conditions of unidirectional stream flow over a planar bed (at a constant flume slope). In his flume setting, four sediment types (amber, lignite, granite and barite), with a range of densities (1.06–4.25 g cm^{-3}) and submerged weights were used. Experiments of each sediment type were repeated with four different slopes. Taking into account a series of physical properties of fluid and sediment, Shields expressed the threshold of sediment motion as a ratio of the critical shear stress to the immersed weight of the grains, which

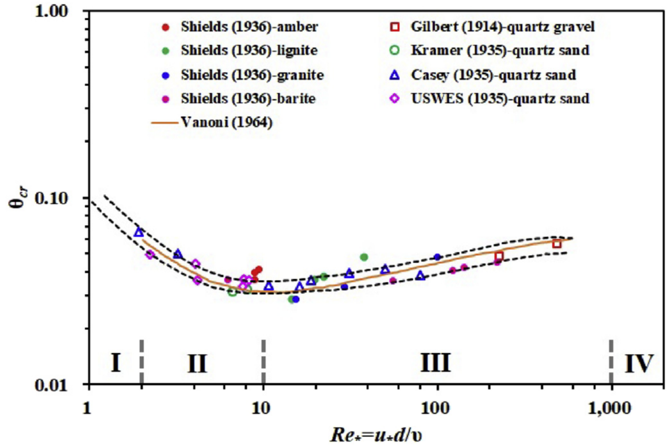

Fig. 2. The original Shields curve as interpreted by a narrow band (dashed line) and four subdivided regions, and the solid line was defined by Vanoni (1964) (Adopted from Miller et al., 1977).

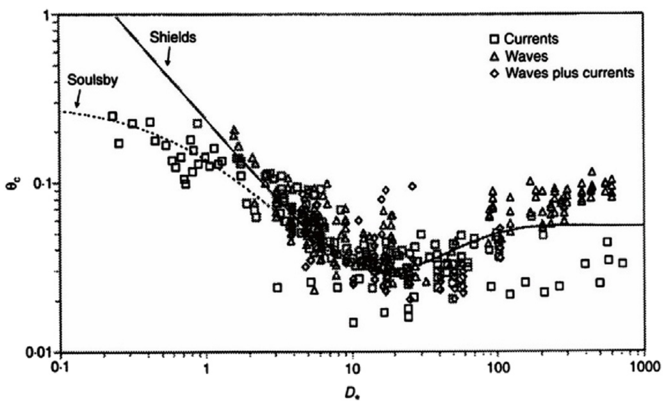

Fig. 3. The dimensionless grain size (D_*) versus critical Shields parameter (θ_{cr}), under the conditions of currents, waves, and combined waves and currents (adopted from Soulsby, 1997).

can be expressed in dimensionless form as:

$$\theta_{cr} = \frac{\tau_{cr}}{(\rho_s - \rho)gd} \tag{3}$$

where θ_{cr} is the critical Shields parameter, τ_{cr} is the critical shear stress, and ρ_s and ρ are density of sediment grains and fluid, respectively. The values of critical Shields parameter was expressed as a function of the grain Reynolds number, defined by:

$$Re_* = \frac{u_* d}{\upsilon} \tag{4}$$

where Re_* is the grain Reynolds number and $u_* = (\tau_{cr}/\rho)^{1/2}$ is the shear velocity.

Based on curve fitting of the measured data and previous supplemental data (Gilbert, 1914; Casey, 1935; Kramer, 1935; USWES, 1935), the well-known Shields curve was generated and reproduced as Fig. 2. The Shields curve should be a general curve since it includes a number of the physical and dynamic parameters of the fluid and sediment. However, the data set showed considerable scatter and could be interpreted as a narrow band rather than a well-defined curve (Buffington, 1999). As shown in Fig. 2, sediment grains move above this band, whereas the sediment grains will not experience motion below it. Moreover, the Shields curve presented a relationship between θ_{cr} and Re_* for four subdivided regions (Fig. 2): in region I ($Re_* < 2$), θ_{cr} increases with decreasing Re_*, reaching a maximum value of approximately 0.1 at $Re_* \approx 1$; Paphitis (2001) extended the Shields curve and suggested a maximum value for θ_{cr} of ~0.2 at $Re_* \approx 0.01$. Within region II ($2 < Re_* < 10$), the threshold curve has a negative slope of −0.50 (approximately 45°); Miller et al. (1977) identified a gentler slope of −0.41, whereas a steeper slope was suggested by Paphitis (2001) with a value of −0.84. In Region III ($10 < Re_* < 1000$), a minimum value of θ_{cr} (~0.033) is found at $Re_* \approx 10$. Miller et al. (1977) and Paphitis (2001) presented a minimum value closer to 0.023 and 0.018 at $Re_* \approx 20$ and 17, respectively. The threshold curve rises from the minimum value at a slope of 0.18 (approximately 10°), which is lower than the slope of 0.40 (approximately 22°) presented by Paphitis (2001). Within region IV ($Re_* > 1000$), θ_{cr} becomes independent of Re_* and the value of θ_{cr} becomes a constant of ~0.06. Other values proposed for the constant θ_{cr} include 0.015, 0.009, 0.007, 0.045, 0.052–0.086 and 0.0475 (Bogardi, 1965; Helland-Hansen, 1971; Paintal, 1971; Miller et al., 1977; Buffington and Montgomery, 1997; Paphitis, 2001, respectively).

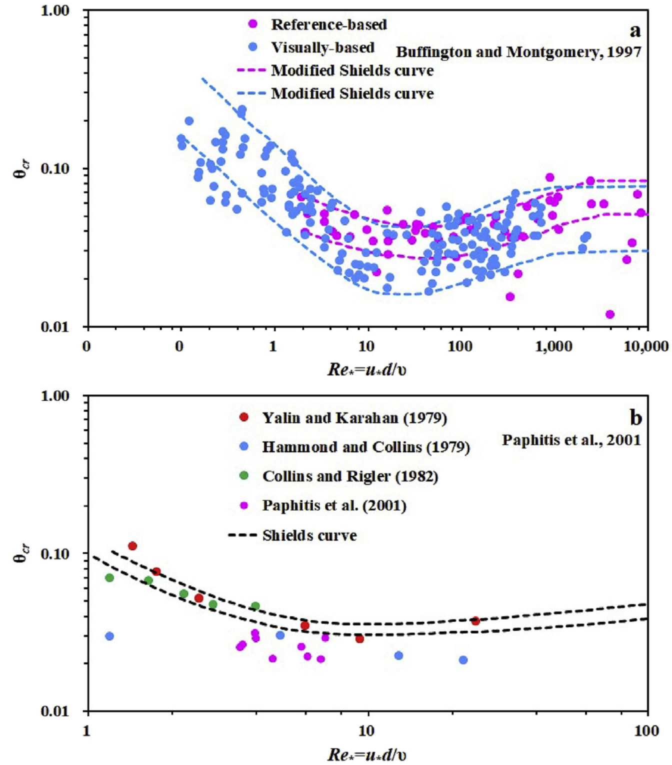

Fig. 4. The Shields curve with some of the additions, revisions and modifications using additional data sets: (a) a revised version of the Shields curve defined by Buffington and Montgomery (1997), based upon threshold data derived through the use of reference transport rate or visual definitions; and (b) the relationship between grain Reynolds number and critical Shields parameter with additional data from Paphitis et al. (2001).

3. The family of Shields curves

3.1. The interpretation of the Shields curve

A drawback of the Shields curve is that the critical shear stress or velocity (τ_{cr} and u_*) appears on both abscissa and ordinate of the Shields curve. For this reason, the critical shear stress cannot be directly determined from the original Shields curve, but requires an iterative process. There are several methods for direct determination of the critical shear stress without iterative calculations. Vanoni (1964) proposed an additional parameter incorporating the properties of fluid and sediment, which is expressed in a non-dimensional form:

$$\frac{d}{\upsilon}\left[\frac{0.1(\rho_s - \rho)gd}{\rho}\right]^{1/2} \tag{5}$$

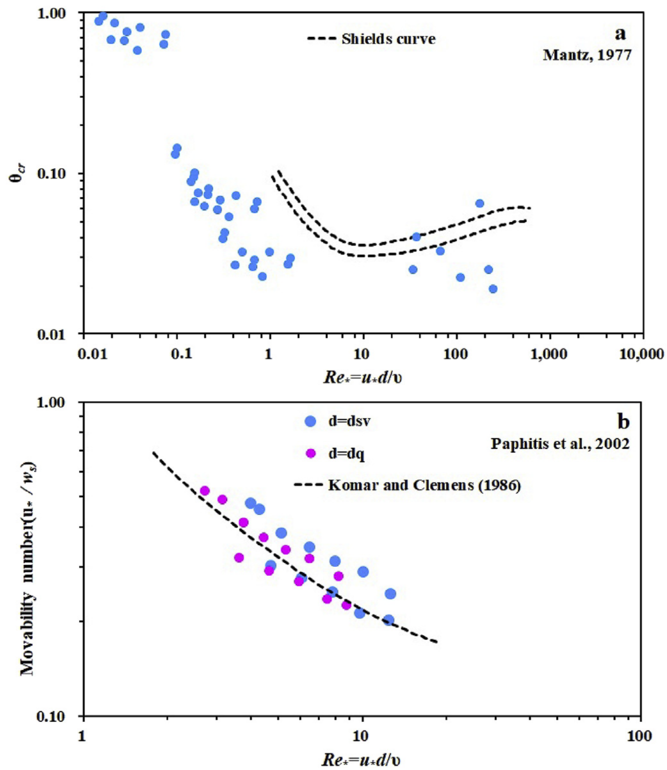

Fig. 5. (a) The Shields curve was extended for smaller grain sizes, defined by Mantz (1977), by investigating cohesionless flaky sediments; (b) The relationship between the grain Reynolds number and the Movability number (u_*/w_s, w_s is the settling velocity of particles), defined by Komar and Clemens (1986) and Paphitis et al. (2002) based on threshold data derived assuming $d = d_{sv}$ (sieve diameter) or $d = d_q$ (settling diameter).

The Vanoni parameter intersects with the Shields curve and provides a direct method to calculate the critical shear stress. In addition, Vanoni (1964) modified the narrow band of Shields curve to a single line for convenient quantitation (Fig. 2).

Yalin (1972) developed the Yalin parameter ($\sqrt{\Xi}$) to eliminate u_* from the abscissa, representing a combination of the critical Shields parameter and grain Reynolds number:

$$\sqrt{\Xi} = \frac{Re_*}{\sqrt{\theta_{cr}}} = \left[\frac{(\rho_s - \rho)gd^3}{\rho\upsilon^2}\right]^{1/2} \tag{6}$$

Equation (6) permits the Yalin parameter to be calculated from the known parameters of fluid and sediment. The Yalin curve (log plot of θ_{cr} and $\sqrt{\Xi}$) has the same general shape as the Shields curve. A slightly different combination of θ_{cr} and Re_* was proposed by Madsen and Grant (1976), and is expressed by $Re_*/\ 4\sqrt{\theta_{cr}}$, which also eliminates the inconvenience of τ_{cr} or u_* appearing on both axes. In addition, the difficulty can also be overcome by the use of a dimensionless grain size (D_*), according to Van Rijn (1993):

$$D_* = \left[\frac{Re_*^2}{\theta_{cr}}\right]^{1/3} = \left[\frac{g(s-1)}{\upsilon^2}\right]^{1/3} d \tag{7}$$

where s = ρ_s/ρ is the ratio of sediment density to the fluid density. The plot of θ_{cr} versus D_* (Fig. 3) has been recommended to determine the critical shear stress, due to its convenient use in practical applications (Soulsby, 1997; Beheshti and Ataie-Ashtiani, 2008). Other convenient threshold curves have been developed since Shields (1936), but these are less general in their application, due to the assumptions made in defining the threshold conditions, e.g. those by Inman (1949, u_* versus d), Lane (1955, τ_{cr} versus d), Sundborg (1956, u_{100} versus d) and Bagnold (1963, θ_{cr} versus d).

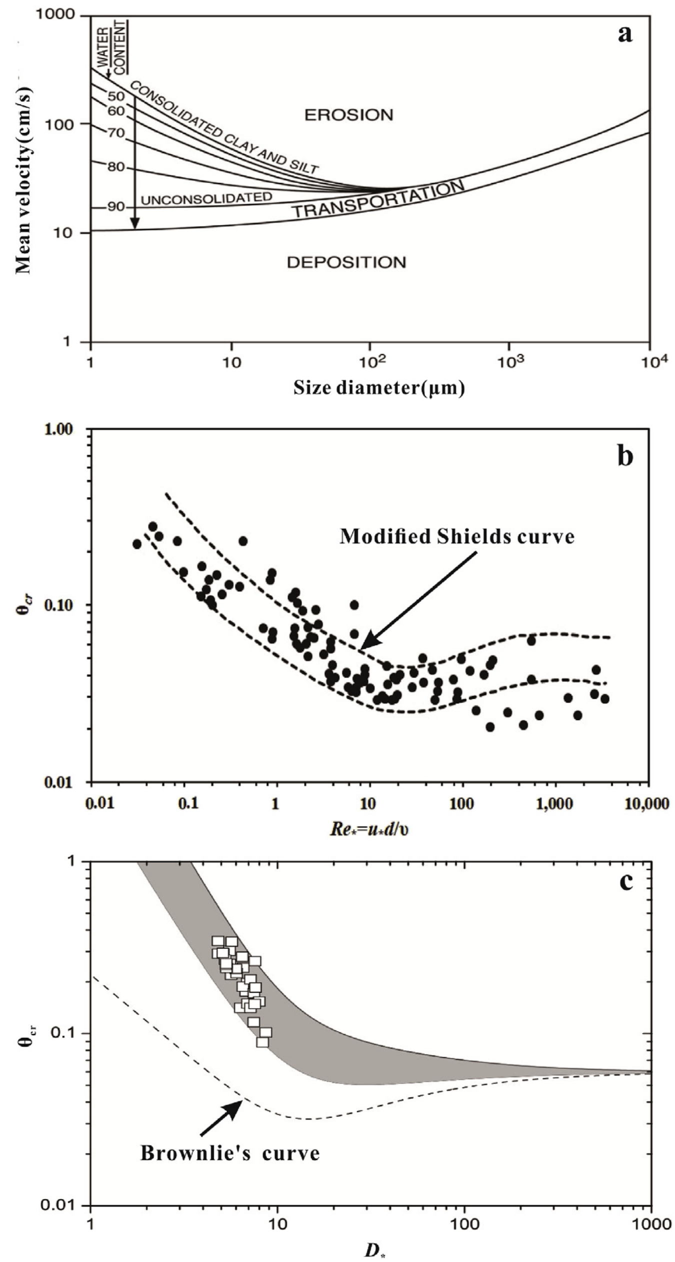

Fig. 6. a) The Postma (1967) curve of thresholds for erosion and deposition according to particle size. b) A modified Shields curve proposed by Miller et al. (1977). c) A modification to the original Shields curve defined by Righetti and Lucarelli (2007): open squares are experimental data, dashed curve is Brownlie's curve (Brownlie, 1981, who suggested an expression for the function of θ_{cr}). Grey area indicates the region in which the experimental data are included.

3.2. The effects of grain size distribution

The flume experiments for the establishment of the Shields curve were conducted with two conditions or limitations: (1) sediment particles used in experiments were spherical and of nearly uniform grain, so the effects of grain size distribution and grain shape cannot be evaluated; and (2) the particles used for the experiments were non-cohesive, i.e., the cohesiveness of fine-grained sediment was not included. However, these two factors are of great importance to threshold conditions (Miller et al., 1977; Paphitis, 2001; Grabowski et al., 2011; Dorrell et al., 2018). Thus, additional flume experiments were carried out to include these factors; the original curve was extended and

Table 1
Classification of the intermittent turbulence events. u' and w' represent the turbulence components of the horizontal and vertical velocities, respectively.

Events	Characteristics	Contributions to Reynolds stress
Outward interaction ($u' > 0, w' > 0$)	high-speed outward movement of fluid reflected by the boundary	Negative
Inward interaction ($u' < 0, w' < 0$)	low-speed inward movement fluid being pushed back to the boundary	Negative
Sweep ($u' > 0, w' < 0$)	high-speed inward movement of fluid towards the boundary	Positive
Ejection ($u' < 0, w' > 0$)	low-speed outward movement of fluid from the boundary	Positive

revised with additional data sets (e.g. Miller et al., 1977; Yalin and Karahan, 1979; Buffington and Montgomery, 1997; Paphitis et al., 2001; Righetti and Lucarelli, 2007; Mehta, 2013).

Most natural sediments are composed of a range of grain sizes, and the relative proportions of these different sized grains can substantially affect the sediment threshold. Flume experiments suggested that the threshold for fine-grained sand increased by up to 90% with addition of clay (Mitchener and Torfs, 1996; Panagiotopoulos et al., 1997). In contrast, other studies have found a negative correlation between critical shear stress and sand content (Gerbersdorf et al., 2005). Laboratory and field studies recognized that mixed sediments exhibit different mobility patterns as compared to nearly uniform sized experimental materials, which may explain some of the scattering (Fig. 2) (Miller et al., 1977). In terms of the effects of grain size distribution, only a few researchers provided quantitative evaluations (Einstein, 1950; Vanoni, 1964; Grass, 1970; Mantz, 1973). Egiazaroff (1967) suggested that the original Shields curve should be placed 15–25% higher to compensate for the use of nearly uniform grains. In addition, mean grain size or a characteristic size (for materials consisting a range of grain sizes or sand-mud mixtures) (Wilcock, 1988; Mitchener and Torfs, 1996; Panagiotopoulos et al., 1997; Wu and Yang, 2004) was used to incorporate the effects of grain size distribution. For example, Buffington and Montgomery (1997) revised the original Shields curve based upon the threshold data of three grain size distribution types (i.e. surface, sub-surface, and laboratory mixture) (Fig. 4a). The contribution of Paphitis et al. (2001) was to assess the threshold of natural sand-sized sediments (subrounded, cohesionless quartz grains with mean grain sizes from 0.315 mm to 0.513 mm) under different flow conditions; the results show a slight overestimation of the threshold when using the Shields curve (Fig. 4b).

3.3. The effects of grain shape

Natural sediments often consist of mixtures with different sphericity and roundness values. The various grain shapes likely lead to differences in sediment thresholds (Briggs et al., 1962; Collins and Rigler, 1982; Buffington et al., 1992; Carling et al., 1992). A number of shape factors have been defined, e.g. sphericity, roundness, rollability, angularity and triaxial particle diameters (Morris, 1957; Carling, 1983; Komar and Li, 1986; Paphitis et al., 2002). None of these shape factors has gained universal approval; hence, they were not incorporated into the Shields curve as an independent variable. In order to assess shape effects, non-spherical, angular particles have been used in flume experiments. Mantz (1977) extended the original Shields curve for smaller grain sizes based on six grades of fine-grained, cohesionless flaky particles (non-spherical grains) under unidirectional flow conditions (Fig. 5a). The magnitude of θ_{cr} is greater or lesser than those for spherical particles depending on how the grain diameter is defined for flaky particles (flake thickness or geometric face diameter). The results indicate the need to define a meaningful grain diameter that incorporates the grain shape effects.

A mathematical-physical model was proposed for the threshold of sediment grains at different sizes, shapes, and densities under unidirectional turbulent flow conditions (Bridge and Bennett, 1992). Moreover, some investigators attempted to link sediment threshold to the settling velocity of particles, incorporating some influence of grain shape effects (Liu, 1957, 1958; Collins and Rigler, 1982; Komar and Clemens, 1986; Paphitis et al., 2002). For example, an alternative approach to the Shields curve was proposed to determine the threshold conditions for any grain shape, through use of the settling velocity of particles (Paphitis et al., 2002, Fig. 5b). However, the problem of settling velocity itself is not simpler than the threshold, and is affected by a wide range of factors including turbulence, suspended sediment concentration (SSC), salinity and sediment properties (size, density, shape and roundness) (Dietrich, 1982; Van Leussen, 1999; Winterwerp, 2002; Shi and Zhou, 2004; Wang et al., 2013; Yang et al., 2016b).

3.4. The effects of cohesiveness

As grain size decreases (typically when grain size is on the order of magnitude of 100 μm or less), the stabilizing effect of cohesive forces due to inter-particles interactions cannot be neglected (Mehta et al., 1989; Dade et al., 1992; Lick et al., 2004). However, the original Shields curve was derived based on non-cohesive particles, so the cohesiveness associated with fine-grained sediments was not included. Subsequently, efforts were made to distinguish cohesive and non-cohesive sediments in relation to the sediment threshold (Otsubo and Muraoka, 1988; Mehta and Lee, 1994; Sanford and Maa, 2001; Jacobs et al., 2011). The erosion behavior of cohesive sediment is more complicated than non-cohesive sediment, due to the different physical, geochemical and biological properties (Mehta et al., 1989; Mitchener and Torfs, 1996; Grabowski et al., 2011). Hjulström (1935) incorporated cohesive effects for very small particles, showing an increasing trend of critical shear velocity with decreasing grain diameter (Fig. 1). Later, Postma (1967) improved the Hjulström curve by incorporating the influence of consolidated and unconsolidated clay and silt (Fig. 6a). Some investigators incorporated the threshold results of cohesive sediment experiments into a Shields-type curve (Dyer, 1986; Righetti and Lucarelli, 2007; Mehta, 2013). Miller et al. (1977) extended Re_* by three orders of magnitude beyond the original Shields curve using selected additional data, and noticed a certain tendency of the threshold curves for cohesive sediment (Fig. 6b). Soulsby (1997) related the critical Shields parameter directly to dimensionless grain diameter, and proposed an analytical formula that fits the original Shields curve, which can be expressed by:

$$\theta_{cr} = \frac{0.24}{D_*} + 0.055\left(1 - e^{-0.020\ D_*}\right) \quad \text{for} \quad D_* > 5 \tag{8}$$

$$\theta_{cr} = \frac{0.30}{1 + 1.2\, D_*} + 0.055\left(1 - e^{-0.020\, D_*}\right) \quad \text{for} \quad D_* \le 5 \tag{9}$$

Equation (8) greatly overestimates the threshold for very fine grain sizes, but Equation (9) fits the curve better. In addition, the Shields curve was extended for the conditions of waves, and combined waves and currents, after a large set of data were tested (Fig. 3). A theoretical threshold model for sediment motion of cohesive-adhesive sediments, based on momentum balance and dimensional considerations, was developed by Righetti and Lucarelli (2007); cohesiveness was parameterized to modify the original Shields curve (Fig. 6c). Recently, Jiang (2019) presented a simple theoretical model for critical shear stress, which models the cohesive force between sediment particles. Apart from the family of Shields curves, some other empirical threshold models have been developed for cohesive sediment, e.g., density model

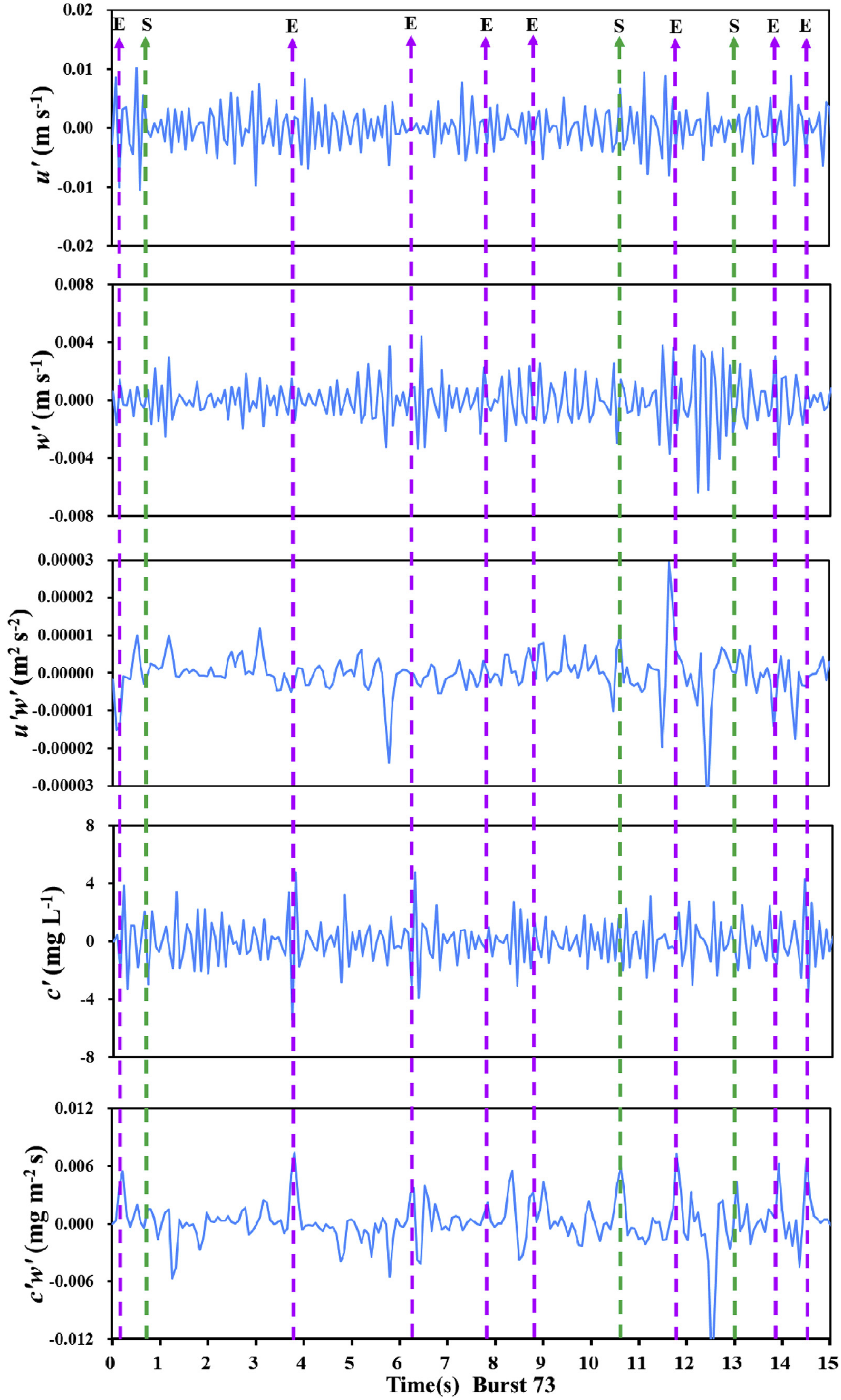

Fig. 7. Time-series of velocities and SSC fluctuations (*u'*, *w'* and *c'*), as well as their products (*u'w'* and *c'w'*), over 15 s of a burst. Major ejection and sweep events are indicated by arrows/dashed lines (magenta arrows: ejection events, green arrows: sweep events) (from Yang et al., 2016a, burst 73, at station D1). (For interpretation of the references to colour in this figure legend, the reader is referred to the Web version of this article.)

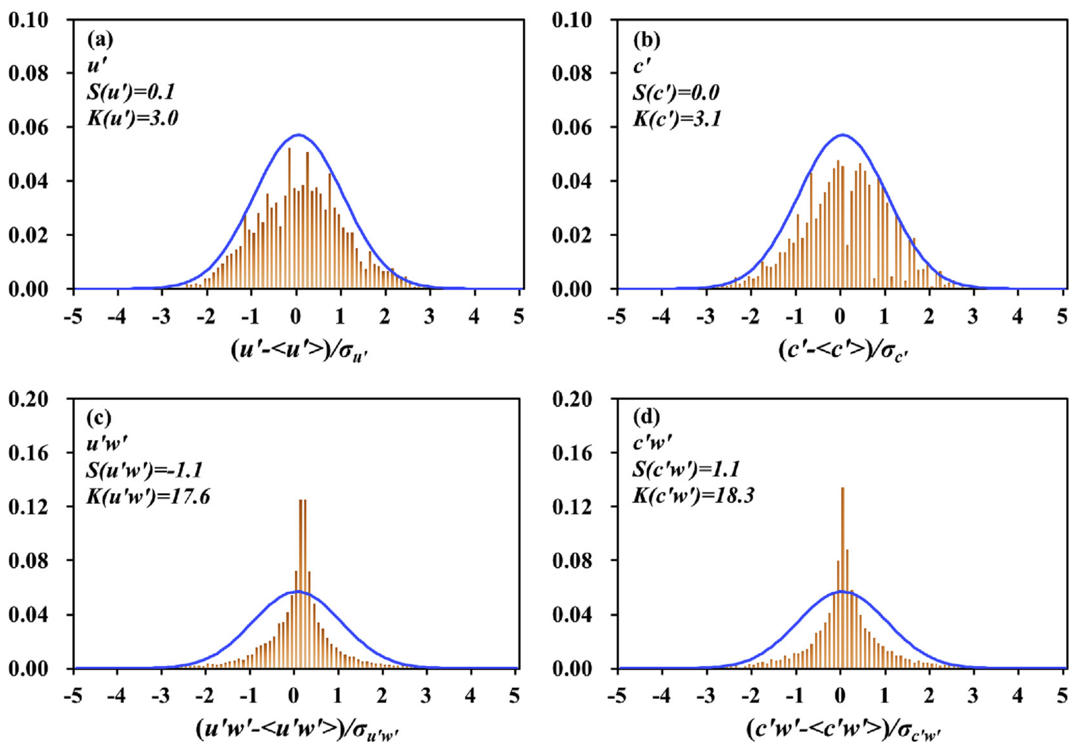

Fig. 8. Probability distributions of (a) *u*', (b) *c*', (c) *u'w*' and (d) *c'w*' in an experimental burst compared with a Gaussian distribution (blue solid lines) (from Yang et al., 2016a, burst 73 at station D1). (For interpretation of the references to colour in this figure legend, the reader is referred to the Web version of this article.)

(Mehta, 1988; Amos et al., 2004), clay content model (Panagiotopoulos et al., 1997) and water content model (Taki, 2001).

3.5. The effects of turbulence

Even when the five variables, as outlined above, are considered, there are still differences between *in situ* measurements and flume experiments. There are differences between the curve-derived critical shear stress and *in situ* measurements (Sternberg, 1971; Tolhurst et al., 1999; Andersen et al., 2007; Salehi and Storm, 2012; Shi et al., 2015). A few field studies undertaken in shallow waters showed that measured threshold for initial sediment motion was well below the Shields curve (O'Callaghan et al., 2010; Salehi and Storm, 2012). This implies that additional factors may contribute to sediment movement. Recently, the effect of turbulence was identified, which was not considered in the original Shields curve (Yang et al., 2016a). Turbulence was originally treated as a random process, but laboratory studies soon revealed that turbulence has an intermittency pattern, associated with a series of well-organized spatial and temporal motions, i.e., “bursting” events (Kline et al., 1967; Grass, 1971). According to the quadrant analysis of turbulent fluctuations (*u*', *w*'), four types of burst events were identified, e.g. ejections, sweeps, outward and inward interactions (Table 1) (Corino and Brodkey, 1969; Heathershaw, 1974).

The discovery of the turbulent bursting phenomenon led investigators to study the role of turbulence on sediment threshold. Studies including laboratory experiments and field observations have shown that sediment resuspension is controlled largely by a sequence of intermittent turbulence events within the bottom boundary layer (McCave, 1976; Heathershaw and Thorne, 1985; Yuan et al., 2009; Kassem et al., 2015). Ejections and sweeps are the two main phases, contributing the largest part of the Reynolds stress, while outward and inward interactions are two much weaker phases (Willmarth and Lu, 1972; Gordon, 1974; Dyer, 1986). In addition, ejection events are associated with suspended sediment transport, and sweep events are related to bedload transport (Heathershaw and Thorne, 1985; Soulsby et al., 1994; Cellino and Lemmin, 2004). Other studies suggested that outward interactions also contribute appreciablly to sediment suspension (Thorne et al., 1989; Nelson et al., 1995). Field studies in tidally- or wave-dominated environments support the laboratory experiments that ejection and sweep are the two main events (Kularatne and Pattiaratchi, 2008; Yuan et al., 2009; Kassem et al., 2015; Yang et al., 2016a; Salim et al., 2018). Records of *u'*, *w'* and *c'* (the fluctuations of SSC), as well as their products *u'w'* and *c'w'* in a tidally dominated environment, give a good indication of the ejection and sweep events (Fig. 7; Yang et al., 2016a). In addition, the probability distributions of *u'*, *w'*, and *c'* were quasi-normal (Fig. 8a and b), whereas the distributions of *u'w'* and *c'w'* had high kurtosis values (Fig. 8c and d), indicating the intermittent nature of turbulences. Thus, sediment suspension models should incorporate the effects of turbulence (e.g. Bridge and Bennett, 1992; Zanke, 2003; Wu and Jiang, 2007).

4. Discussion

4.1. Scale effects of turbulence

The preceding sections examined the factors that influence the threshold of sediment motion in relation to the improvement of the original Shields curve. To this point, the critical Shields parameter has been found to be a function of at least six variables, e.g. grain Reynolds number, grain size distribution, sphericity, roundness, cohesiveness and the scale effects of turbulence, but so far the Shields curves have not included the effects of turbulence.

Recently, on the mega-tidal Jiangsu coast, where resuspension processes dominate, *in situ* measurements of the nearly synchronous variations between SSCs and τ_c can be used to identify the critical shear stress for erosion (Fig. 9; Yang et al., 2016a). The results revealed that the measured threshold for initial sediment motion is well below the value predicted by the Shields curve, with a difference between 30% and 83% (Fig. 10). Similar results were also found in previous studies (O'Callaghan et al., 2010; Salehi and Storm, 2012). This effect becomes more obvious when the mean current is below the critical condition for sediment transport. In more detail, the scale effects of turbulence are

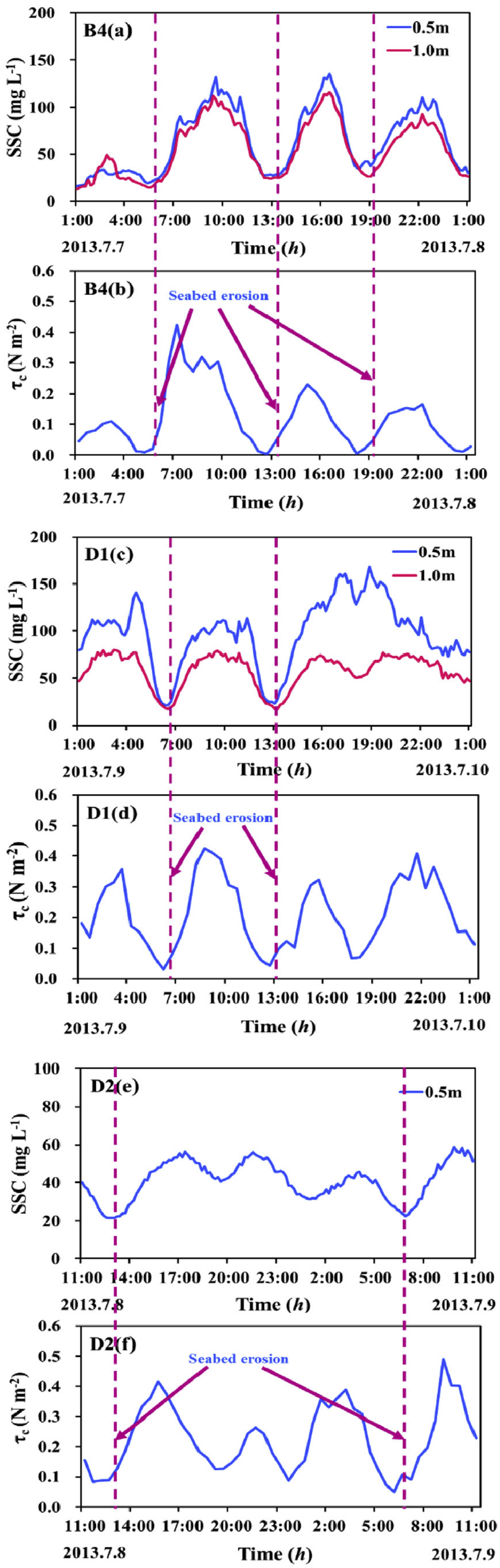

Fig. 9. Tidal variability shown for B4, D1 and D2 of: (a, c, and e) SSC; and (b, d, and f) near-bed shear srtess at a height of 0.5 and/or 1.0 m above the seabed. Vertical dashed lines show a seabed erosion (resuspension) occurrence (from Yang et al., 2016a). See Fig. 11 for the site locations.

related to the temporal and spatial structures of turbulence: the magnitude of instantaneous velocity fluctuations varies in time and in location (Heathershaw, 1974; Cellino and Lemmin, 2004). For the same mean current velocity or near-bed shear stress, the addition of the fluctuation magnitudes may influence the threshold. For instance, in flumes the limited water depth does not allow intense fluctuations, but in coastal waters with larger spatial scales and stronger hydrodynamic forcing, the magnitude of fluctuations may be enhanced (Couturier et al., 2000; Yang et al., 2016a). As a result, the threshold measured by mean bed shear stress would be higher in the flume, whereas in the coastal waters, resuspension takes place even if the bed shear stress is below the Shields curve.

As shown in Fig. 7, the turbulence signals of Jiangsu coastal waters exhibit a high degree of variability and intermittency over time (Yang et al., 2016a). Due to this irregular variability of turbulence structure, there is little consensus on the most appropriate method to identify or quantify the intermittency of turbulence from the raw measured records (Farge, 1992; Keylock, 2007). Under such circumstances, wavelet transforms provide a more effective and intuitive way to visualize the intermittency of turbulence in both time and space (Salmond, 2005). For instance, large ejection and sweep events of $u'w'$ and $c'w'$ can be identified clearly in the Jiangsu coastal waters, corresponding to the red plume streaks shown in Fig. 11 (Yuan et al., 2009; Yang et al., 2016a). Further laboratory and field studies (Salim et al., 2017, 2018; Xiong et al., 2017) highlighted the importance of the scale effects of turbulence on the threshold of sediment motion. However, two critical questions have been raised: how to quantify the scale effects of turbulence, and how to account for different scale effects of turbulence in the Shields curves?

In the Shields curve, mean bed shear stress is considered as the only integral parameter for determining the hydraulic forces acting on particles, but for the same bed shear stress, the forces on particles may differ due to the additional spatial or temporal accelerations (e.g. Nelson et al., 1995; Vollmer and Kleinhans, 2007; O'Callaghan et al., 2010). Taking into account the grain contact angle and the fluctuation velocity, analytical formulations (Equations 15b and 15cin Zanke, 2003) for the Shields curve were developed, indicating that the threshold of sediment motion is reduced due to turbulence enhancement. In treating the fluctuation velocity for initiating motion, the Gaussian probability distribution was used by Zanke (2003). However, measurements soon revealed a non-Gaussian distribution (Frenkiel and Klebanoff, 1967; Nakagawa and Nezu, 1977). Some investigators suggested that higher-order moments (mean velocity and the velocity fluctuations as the first- and second-order moment) should be incorporated into the probability distribution, e.g. the third moment (skewness factor) in relation to relative importance of particular burst events, and the fourth-moment (flatness or kurtosis) associated with turbulence intermittency (Frenkiel and Klebanoff, 1973; Durst et al., 1987; Dittrich et al., 1996; Wu and Yang, 2004). Thus, a number of non-Gaussian probability distributions have been used to describe the velocity fluctuations or Reynolds stress, e.g. Gram-Charlier distribution (Frenkiel and Klebanoff, 1967), seven-parameter general distribution (Barndorff-Nielsen, 1979), hyperbolic distribution (Durst et al., 1987) and the lognormal distribution (Wu and Lin, 2002). Previous studies have shown that the Gram-Charlier probability distribution (fourth-order) satisfactorily describes the distribution of near-bed velocity fluctuations, since it includes the effect of turbulent bursting (e.g. Frenkiel and Klebanoff, 1973; Wu and Yang, 2004; Bose and Dey, 2013). Recently, direct numerical simulation (DNS), taking into account the effects of turbulent structures, has been adopted to predict the threshold of sediment motion (Schmeeckle, and Nelson, 2003; Ji et al., 2013; Mathis et al., 2014). While DNS has the potential to predict the threshold of sediment motion in relation to turbulent bursting events, its application on large-scale, complex flows remains limited (Mathis et al., 2013).

The scale effects of turbulence are associated with water depth and

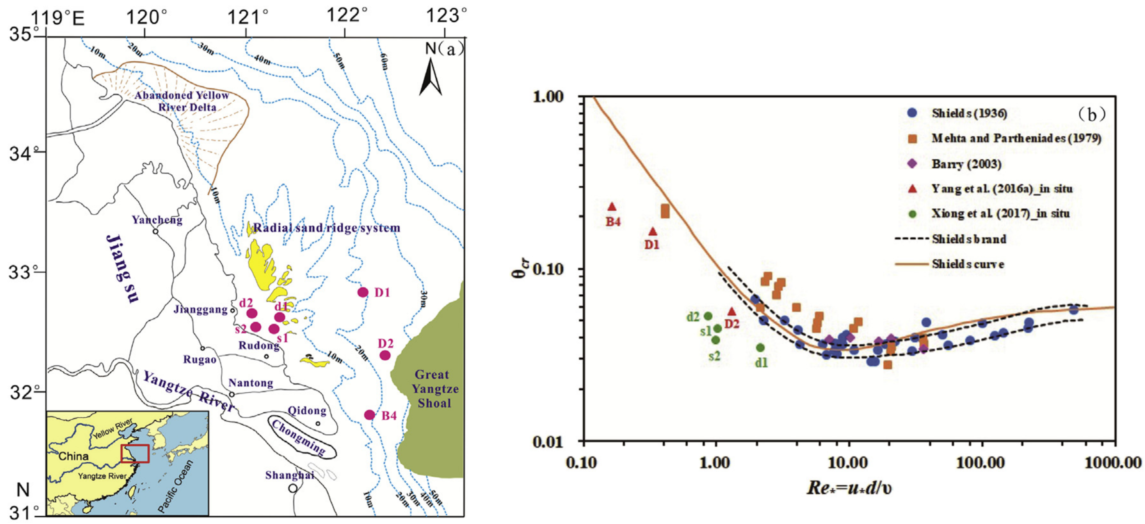

Fig. 10. (a) Map of the locations of the observation sites (red circled dots) in the southern Yellow Sea, China; Tripods were deployed at B4, D1, D2, d1, s1, d2 and s2 stations. (b) A comparison of critical shear stress for seabed erosion derived by *in situ* measurements and Shields curve, with additional data from Mehta and Partheniades (1979) and Barry (2003). (For interpretation of the references to colour in this figure legend, the reader is referred to the Web version of this article.)

hydrodynamic conditions (e.g. tidal currents, tidal types and waves). However, these studies are still limited to similar scales of water depth and hydrodynamic conditions (e.g. Yang et al., 2016a; Salim et al., 2017, 2018; Xiong et al., 2017). In particular, little is known about the turbulence processes at extremely shallow water stages (i.e. when the water depth is much smaller than the thickness of bottom boundary layer) in relation to the threshold conditions. It is during the extremely shallow water stages that sediment dynamic processes are likely to differ from those during deeper flows (Fagherazzi and Mariotti, 2012; Zhang et al., 2016; Shi et al., 2017). Intertidal flats and tidal creeks represent examples of extremely shallow water environments. Observations from the Wanggang tidal flat, Jiangsu coast, show that towards the end of an ebb tide phase, the bed surface and tidal creeks are subject to water flows with low current speed (0.1 m/s in magnitude) and extremely shallow water depth (1 cm in magnitude). As a result, flat-topped ripples (Fig. 12a) and plane bed (Fig. 12b) are formed on the lower parts of the intertidal flat, whilst small-scale secondary creeks develop at the bottom of major creeks over the upper part of the intertidal flat (Fig. 12c). In these cases, the flow structure within the bottom boundary layer appears to be maintained, with the u_{100} value derived being applicable to the calculation of the critical shear velocity. Tidal surges occurring over the middle part of the intertidal flat (Fig. 12d) are another type of behavior for the extremely shallow water processes. In this case, the height of the tidal surge ($H_b = 4z_0$; z_0: bed roughness length) is equivalent to the critical water depth, and u_{100} rises sharply, implying a collapse of the Von Kármán-Prandtl flow structure (Gao, 2010). This means that the calculation of u_{100} based on the Von Kármán-Prandtl model is no longer applicable. Thus, in the future more attention should be paid to the turbulence structure of the extremely shallow water stages and its influence on sediment threshold.

In the future, additional laboratory experiments and *in situ* measurements under different water depths and hydrodynamic conditions should be carried out to obtain information on the relationship between the scale effects of turbulence and water depth and hydrodynamic conditions. In addition, process-based numerical models at different spatial scales are required to assess the effects of turbulence on sediment threshold, and the data from *in situ* measurements can be compared to model predictions. On this basis, combined with the advances of theoretical framework of the threshold of sediment motion, it will be possible to construct a dimensionless variable in line with the Shields parameter related to the turbulence effect, and to derived a new Shields curve.

4.2. Observational techniques

Over the last 50 years, various innovative techniques have been developed to measure and calculate currents, waves and SSCs. Therefore, the turbulence structures and their relationship to sediment movement can be defined by *in situ* measurements, or numerical modeling. In the early days, the near-bed turbulence structures associated with a sequence of well-organized events were investigated in the laboratory using flow visualization techniques (e.g. Kline et al., 1967; Grass, 1971; Nychas et al., 1973). Turbulence bursting was also observed in the sea (e.g. Gordon, 1974; Heathershaw, 1974). The first benthic tripod developed by Sternberg and Creager (1965) was equipped with a current rotor and vane (for current speed and direction), and contributed many important advances in the threshold of sediment motion (Sternberg, 1971, 1972). However, attempts to link the turbulence bursting and sediment movement at the seabed were limited, due to the poor temporal resolution of observational techniques. With the development of passive acoustic techniques, it is possible to observe sediment movement with a temporal resolution comparable to high frequency turbulence in flow. In the 1980s, a significant advance in the measurement of SSCs and detailed vertical profiles of current velocity was originally derived from the use of optical backscattering sensors (OBS, 2Hz) (Downing et al., 1981) and acoustic Doppler current profilers (ADCPs) (Thomson et al., 1989). Once adapted to the near bed measurement, high-temporal resolution current velocities and SSCs were measured simultaneously to investigate the role of turbulent bursting on sediment movement.

In the early 2000s, single-point acoustic Doppler velocimeters (ADVs) became the preferred current sensor, largely owing to their accuracy and high frequency sampling rate (up to 20 Hz), and relatively low power usage (Kim et al., 2000). Although the OBS has become the standard sensor for measuring SSC, high-frequency acoustic backscatter sensors (ABS) are also used to provide the profile of SSCs and the sizes of suspended sediment (Thorne et al., 1993). In addition, high frequency SSCs can be determined by ADV acoustic backscatter through calibration (Yang et al., 2016b). More recently, the emergence of high-order temporal resolution instruments (e.g. ADV, up to 64 Hz) has been used to measure both SSC and current velocity, which facilitates a deeper understanding of the turbulence process (Salim et al., 2017). However, there is still uncertainty in the field measurements in terms of the frequency and quality of the measured data, due to the complex natural environment and the instrument itself (e.g. noise, the

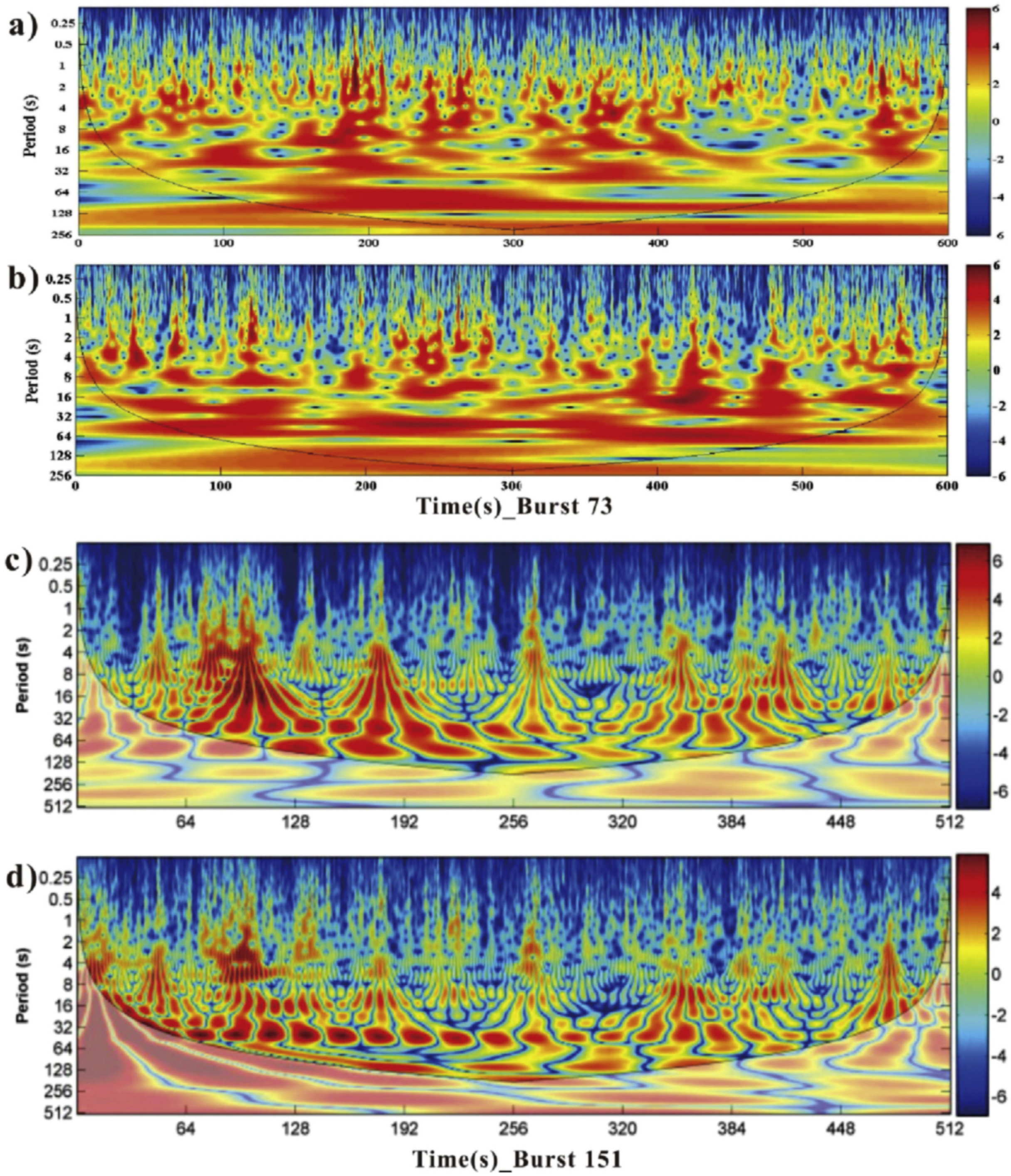

Fig. 11. A comparison of wavelet power spectra (W/Hz, using the Morlet wavelet) of variables: (a and c) *u'w'*; and (b and d) *c'w'*. From Yang et al. (2016a) and Yuan et al. (2009).

interaction of multiple probes). For instance, high frequency data obtained from ADVs in unsteady estuary flows cannot be analyzed in an over-simplified way, and post-processing techniques are needed to check the quality of the dataset (Chanson et al., 2008; Yang et al., 2016b).

For these reasons, it is necessary to improve the accuracy and frequency of *in situ* measurements. First, new observational techniques should be developed covering higher frequency (e.g. Nortek Vectrino Plus with a maximum sampling rate of 200 Hz; Sellar et al., 2015), with an improved ability for extreme environments (e.g. RBR Wirewalker wave-powered profiling system). Second, optimal configuration of the instrument involved in the observation system is required (e.g. sampling rate, vertical resolution, position of probes) to reduce the impact of the instrument itself on the flow structure. Third, new data post-processing methods are needed to ensure data quality, e.g. tilt angle of sensor, signal-to-noise ratio, correlation analysis, the interaction of multi probes and other unpredictable disturbance (Lu et al., 2012; Yang et al., 2016b). Finally, big data methods must be developed to use the global databases of high frequency flow velocities, SSCs and transport rates in various environments to assess the effects of turbulence on sediment threshold and to construct a dimensionless variable associated with turbulence effects. For instance, a global seismic dataset collected

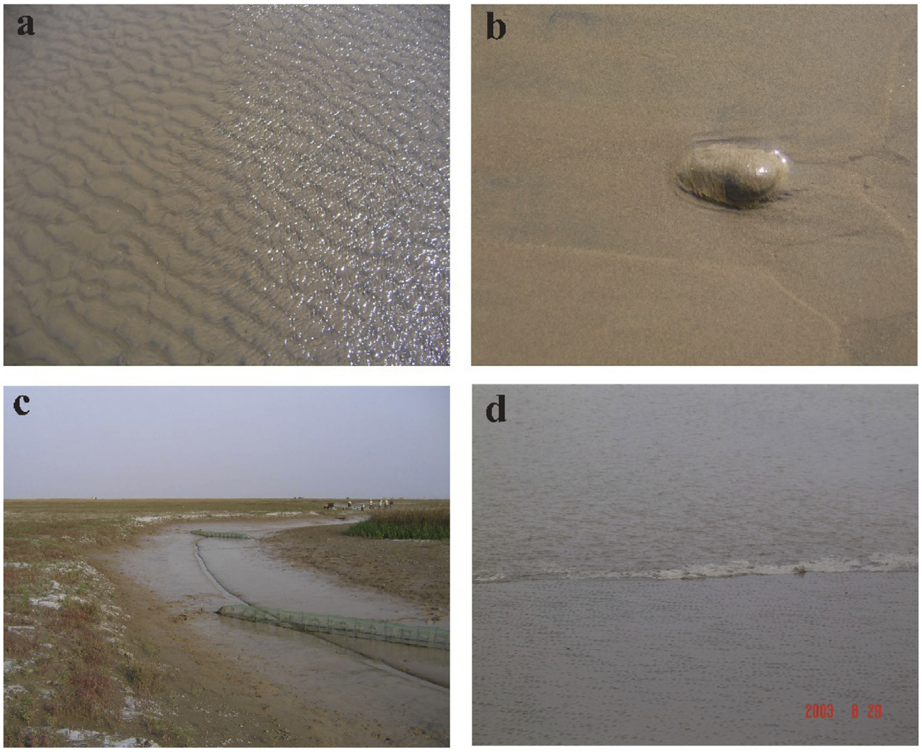

Fig. 12. Sedimentological and morphological characteristics associated with the bottom boundary layer processes of extremely shallow water depths, on the Wanggang tidal flat, Jiangsu coast, China (Gao, 2010): a) flat-topped ripples (location: 120°49.6′E, 33°13.8′N; observation time: 3rd May 2008); b) plane bed, the *Bullacta exarata* shell is 4 cm in length (location: 120°49.6′E, 33°13.8′N; observation time: 3rd May 2008); c) a secondary tidal creek at the bottom of a major tidal creek (location: 120°45.0′E , 33°14.6′N; observation time: 15th May 2006); and (d) Tidal surges (height 5–10 cm) over the middle part of the intertidal flat (location: 120°48.5′E , 33°14.0′N; observation time: 29th June 2003).

Table 2
The influence of several factors on the original Shields curve.

Factors	The influence on the original Shields curve	References
Grain Reynolds number	The critical Shields parameter is a function of grain Reynolds number, which expressed implicitly the threshold for non-cohesive spherical particles with the same diameter	Shields (1936)
Grain size distributions	A slight overestimation of the threshold of natural sediments, as compared to the original Shields curve	Paphitis et al. (2001)
Sphericity/Roundness	Grain shape factor represents both sphericity and roundness effects, grain shape has no effect on θ_{cr} at low grain Reynolds numbers, whereas θ_{cr} decreases as roundness and sphericity decreases for larger grain Reynolds numbers	Bridge and Bennett (1992)
Cohesiveness	Underestimation of the threshold of the cohesive sediments, as compared to the original Shields curve	Righetti and Lucarelli (2007)
Scale effects of turbulence	Overestimation of the threshold, taking into account the effects of burst turbulence, as compared to the original Shields curve	Yang et al. (2016a)
Biology/biogeochemistry	Underestimation of the threshold, taking into account the effects of biological impacts and non-particle components, as compared to the original Shields curve	Winterwerp and van Kesteren (2004); Chen et al. (2017)

over the last 40 years has been used to investigate the relationship between volcanic eruptions and seismic activity around volcanoes, and clearly reveals that volcanic eruptions trigger moderate earthquakes (Nishimura, 2018). Big data methods can also facilitate a greater understanding of the theoretical framework of the threshold of sediment motion.

4.3. Other factors: biological and non-particle components

In addition to the factors listed in Table 2, other factors need similar considerations, e.g. biological impacts and non-particle components in sediments (Kaller and Hartman, 2004; Winterwerp and van Kesteren, 2004; Grabowski et al., 2011; Malarkey et al., 2015).

From microscopic (e.g. bacteria and diatoms) to macroscopic (e.g. bivalves and echinoderms), all sediment is inhabited by organisms of the seabed, which can alter sediment properties by bioturbation (physical modification), biostabilization and biodestabilization (biological modification of the seabed) (Black et al., 2002). The formation of biofilms is a representative example of biostabilization that can increase the erosion threshold. Biological forms influence the sediment threshold through the processes of bioturbation, feeding, egestion and creation (e.g. burrows, roots, or extracellular polymeric substances) (De Deckere et al., 2001; Andersen et al., 2005). Their impact is controlled mainly by the organism size and abundance, the frequency and intensity of their behaviors, the properties of the biogenic structures and the interactions with others within the biological community (Grabowski et al., 2011). Regarding the effects of biological forms on sediment threshold, extracellular polymeric substances (EPS) are commonly cited examples (Paterson, 1997; Tolhurst et al., 2003, 2008; Malarkey et al., 2015). Laboratory and field studies have shown that EPS-related surficial biofilms increase the erosion threshold for both cohesive and non-cohesive sediment. Likewise, the total carbohydrate fraction (as a measure of EPS) has been negatively correlated with the threshold, increasing the stability of the sediment by 120–900% (Friend et al., 2003; Tolhurst et al., 2003, 2008). Recently, a comparison of the erosion thresholds (Shields parameter) for biosediment and clean sediment was made, and a significant increase in Shields parameters was observed in the bio-sedimentation systems (Chen et al., 2017). Further attempts should incorporate the biological effects as a dependent variable (e.g. a bed-age associated depth-dependent parameter, Chen et al., 2017) into the Shields curve.

Non-particle components in sediments, such as dissolved ions (i.e. sodium adsorption ration and salinity), pH and metals (i.e. soluble metals, divalent metal ions and metal contamination) affect the sediment erodibility through biogeochemical processes (Winterwerp and van Kesteren, 2004; Grabowski et al., 2011). The adsorption and mechanical properties of EPS, which affects sediment thresholds, are in turn affected by the concentration of divalent cations, (e.g. Tolhurst et al., 1999; De Brouwer et al., 2002). For example, high pH can increase the threshold due to a decrease in H^+ ions (Winterwerp and van Kesteren, 2004). Although there is a correlation between sediment thresholds and one or several non-particle components, our knowledge of how to parameterize these effects (Grabowski et al., 2011) and how they relate to the Shields curve is still insufficient. Here, the establishment of laboratory and field observations containing several key non-particle components in various environments are needed. On this basis, a concentration-dependent variable representing the effects of non-particle components may be identified for the Shields curve.

5. Conclusions

(1) In this study, the Shields curve and its evolution were re-examined, and important factors related to the critical Shields parameter were synthesized, i.e. grain Reynolds number, grain size distributions, sphericity, roundness, cohesiveness, and the scale effects of turbulence. The turbulence scale factor has not been included in the traditional Shields curves. Turbulence has both temporal and spatial structures, which causes the deviation of *in situ* measurements from theoretical curves. In coastal-shelf waters, resuspension occurs even if the bed shear stress is well below the Shields curve.
(2) The scale effects of turbulence are related to water depth and hydrodynamic conditions (e.g. tidal currents, tidal types and waves). Therefore, laboratory experiments and *in situ* measurements in different water depths and hydrodynamic conditions should be performed to obtain information on the relationship between the turbulence and the threshold. Further, process-based numerical models at different spatial scales should be established to assess the effects of turbulence on sediment threshold, compared against field observations.
(3) Advances in our understanding of turbulence process in the sea are often guided by new data from emerging observational techniques. Uncertainty still exists in field measurements in terms of the frequency and quality of the measured data. Hence, we recommend: (i) development of new observational techniques for higher frequency and improved capability in extreme environments; (ii) establishment of optimal configuration of instruments to reduce the impact of instrument on the flow structure; (iii) development of new data post-processing methods to ensure data quality; and (iv) use of big data methods that cover global databases of high frequency flow velocities, SSCs, and transport rates.
(4) Biological impacts and non-particle components in sediments are also important influencing factors. Quantifying the effect of these factors is crucial to the prediction of sediment transport. Laboratory and field observations should be performed to evaluate these factors in terms of the sediment threshold.

Acknowledgements

This study was supported by the National Natural Science Foundation of China (grant Nos. 41706095, 41625021 and 41530962). YY was supported by the China Postdoctoral Science Foundation (grant No.2017M611495). Part of this study was present in the conference of “Turbulent Mixing and Sediment Transport in the Ocean” (13th September 2016) in Guangzhou, China. Dr. Wenxiang Zhang is thanked for his help with the discussion of section 4.2. We thank the reviewers for their comments on the original manuscript. We are grateful to Editors Andrea Ogston and Jiaxue Wu for improving the scientific content. The authors are grateful to Professor David J.W. Piper for improving the English language usage.

References

Ali, S.Z., Dey, S., 2016. Hydrodynamics of sediment threshold. Phys. Fluids 28 (7), 484–486.
Amos, C.L., Bergamasco, A., Umgiesser, G., Cappucci, S., Cloutier, D., DeNat, L., Flindt, M., Bonardi, M., Cristante, S., 2004. The stability of tidal flats in Venice lagoon-the results of in-situ measurements using two benthic, annular flumes. J. Mar. Syst. 51, 211–241.
Andersen, T.J., Fredsoe, J., Pejrup, M., 2007. *In situ* estimation of erosion and deposition thresholds by Acoustic Doppler Velocimeter (ADV). Estuarine. Coast Shelf Sci. 75 (3), 327–336.
Andersen, T.J., Lund-Hansen, L.C., Pejrup, M., Jensen, K.T., Mouritsen, K.N., 2005. Biologically induced differences in erodibility and aggregation of subtidal and intertidal sediments: a possible cause for seasonal changes in sediment deposition. J. Mar. Syst. 55 (3–4), 123–138.
Bagnold, R.A., 1963. Sedimentation: beach and nearshore processes. In: In: Hill, M.N. (Ed.), The Sea, vol. 3 Interscience Publishers, New York.
Barndorff-Nielsen, O., 1979. Models for non-Gaussian variation, with applications to turbulence. Proc. Roy. Soc. A 368, 501–520.
Barry, K.M., 2003. The Effect of Clay Particles in Pore Water on the Erosion of Sand. PhD Thesis. University of Florida, Gainesville.
Beheshti, A.A., Ataie-Ashtiani, B., 2008. Analysis of threshold and incipient conditions for sediment movement. Coast. Eng. 55 (5), 423–430.
Black, K.S., Tolhurst, T.J., Paterson, D.M., Hagerthey, S.E., 2002. Working with natural cohesive sediments. J. Hydraul. Eng. 128 (1), 2–8.
Bogardi, J.L., 1965. European concepts of sediment transportation. J. Hydraul. Div. 91 (1), 29–54.
Bose, S.K., Dey, S., 2013. Sediment entrainment probability and threshold of sediment suspension: exponential-based approach. J. Hydraul. Eng. 139 (10), 1099–1106.
Bridge, J.S., Bennett, S.J., 1992. A model for the entrainment and transport of sediment grains of mixed sizes, shapes, and densities. Water Resour. Res. 28 (2), 337–363.
Briggs, L.I., Mcculloch, D.S., Moser, F., 1962. The hydraulic shape of sand particles; errata. J. Sediment. Res. 33 (2), 482.
Brownlie, W.R., 1981. Prediction of Flow Depth and Sediment Discharge in Open Channels. Rep. No. KH-R-43B. Lab. of Hydraulic Research, California Institute of Technology, Pasadena, Calif.
Buffington, J.M., 1999. The legend of AF Shields. J. Hydraul. Eng. 125 (4), 376–387.
Buffington, J.M., Dietrich, W.E., Kirchner, J.W., 1992. Friction angle measurements on a naturally formed gravel streambed: implications for critical boundary shear stress. Water Resour. Res. 28 (2), 411–425.
Buffington, J.M., Montgomery, D.R., 1997. A systematic analysis of eight decades of incipient motion studies, with special reference to gravel-bedded rivers. Water Resour. Res. 33 (8), 1993–2029.
Cao, Z., Pender, G., Meng, J., 2006. Explicit formulation of the shields diagram for incipient motion of sediment. J. Hydraul. Eng. 132 (10), 1097–1099.
Carling, P.A., 1983. Threshold of coarse sediment transport in broad and narrow natural streams. Earth Surf. Process. Landforms 8 (1), 1–18.
Carling, P.A., Kelsey, A., Glaister, M.S., 1992. Effect of bed roughness, particle shape and orientation on initial motion criteria. In: Billi, P., Hey, R.D., Thorne, C.R., Tacconi, P. (Eds.), Dynamics of Gravel-Bed Rivers. John Wiley, New York, pp. 24–39.
Casey, H.J., 1935. ‘‘Ü ber Geschiebebewegung.’’ Mitteilungen der Preussischen Versuchsanstalt für Wasserbau und Schiffbau. Heft 19 Berlin (in German).
Cellino, M., Lemmin, U., 2004. Influence of coherent flow structures on the dynamics of suspended sediment transport in open-channel flow. J. Hydraul. Eng. 130 (11), 1077–1088.
Chanson, H., Trevethan, M., Aoki, S.I., 2008. Acoustic Doppler velocimetry (ADV) in small estuary: field experience and signal post-processing. Flow Meas. Instrum. 19 (5), 307–313.
Chen, X.D., Zhang, C.K., Paterson, D.M., Thompson, C.E.L., Townend, I.H., Gong, Z., Zhou, Z., Feng, Q., 2017. Hindered erosion: the biological mediation of non-cohesive sediment behaviour. Water Resour. Res. 53 (6), 4787–4801.
Coleman, N.L., 1967. A theoretical and experimental study of drag and lift forces acting on a sphere resting on a hypothetical stream bed. In: Proceedings of the 12th Congress of International Association for Hydraulic Research. 3. pp. 185–192.
Collins, M.B., Rigler, J.K., 1982. The use of settling velocity in defining the initiation of motion of heavy mineral grains, under unidirectional flow. Sedimentology 29, 419–426.
Corino, E.R., Brodkey, R.S., 1969. A visual investigation of the wall region in turbulent flow. J. Fluid Mech. 37 (1), 1–30.
Couturier, M.N.L., Grochowski, N.T., Heathershaw, A., Oikonomou, E., Collins, M.B., 2000. Turbulent and macro-turbulent structures developed in the benthic boundary layer downstream of topographic features. Estuar. Coast Shelf Sci. 50 (6), 817–833.
Dade, W.B., Nowell, A.R.M., Jumars, P.A., 1992. Predicting erosion resistance of muds. Mar. Geol. 105, 285–297.
Dancey, C.L., Diplas, P., Papanicolaou, A., Bala, M., 2002. Probability of individual grain movement and threshold condition. J. Hydraul. Eng. 128 (12), 1069–1075.
De Brouwer, J.F.C., Ruddy, G.K., Jones, T.E.R., Stal, L.J., 2002. Sorption of EPS to sediment particles and the effect on the rheology of sediment slurries. Biogeochemistry 61 (1), 57–71.
De Deckere, E., Tolhurst, T.J., De Brouwer, J.F.C., 2001. Destabilization of cohesive intertidal sediments by infauna. Estuar. Coast Shelf Sci. 53 (5), 665–669.
Dey, S., Sarkar, S., Solari, L., 2011. Near-bed turbulence characteristics at the entrainment threshold of sediment beds. J. Hydraul. Eng. 137 (9), 945–958.
Dietrich, W.E., 1982. Settling velocity of natural particles. Water Resour. Res. 18 (6), 1615–1626.

Dittrich, A., Nestmann, F., Ergenzinger, P., 1996. Ratio of Lift and Shear Forces over Rough Surfaces. Wiley, Chichester, pp. 125–146.
Dorrell, R.M., Amy, L.A., Peakall, J., Mccaffrey, W.D., 2018. Particle size distribution controls the threshold between net sediment erosion and deposition in suspended load dominated flows. Geophys. Res. Lett. 45, 1443–1542.
Downing, J.P., Sternberg, R.W., Lister, C.R.B., 1981. New instrumentation for investigation of sediment suspension in the shallow marine environment. Mar. Geol. 42, 19–34.
Durst, F., Jovanovic, J., Kanevce, L., 1987. Probability density distribution in turbulent wall boundary-layer flows. In Turbulent Shear Flows 5, 197–220 (Springer, Berlin, Heidelberg).
Dyer, K., 1986. Coastal and Estuarine Sediment Dynamics. Wiley, Chichester, pp. 342.
Egiazaroff, I.V., 1967. Discussion of" Sediment transportation mechanics: initiation of motion. J. Hydraul. Div. 93, 281–287.
Einstein, H.A., 1950. The Bed-Load Function for Sediment Transportation in Open Channel Flows. USDA, Soil Conservation Service Tech. Bull. 1026, Washington, DC.
Farge, M., 1992. Wavelet transforms and their applications to turbulence. Annu. Rev. Fluid Mech. 24 (1), 395–457.
Fagherazzi, S., Mariotti, G., 2012. Mudflat runnels: evidence and importance of very shallow flows in intertidal morphodynamics. Geophys. Res. Lett. 39 (14).
Frenkiel, F.N., Klebanoff, P.S., 1967. Higher-order correlations in a turbulent field. Phys. Fluids 10, 507–520.
Frenkiel, F.N., Klebanoff, P.S., 1973. Probability distributions and correlations in a turbulent boundary layer. Phys. Fluids 16 (6), 725–737.
Friend, P.L., Ciavola, P., Cappucci, S., Santos, R., 2003. Bio-dependent bed parameters as a proxy tool for sediment stability in mixed habitat intertidal areas. Cont. Shelf Res. 23 (17–19), 1899–1917.
Gao, S., 2010. Extremely shallow water benthic boundary layer processes and the resultant sedimentological and morphological characteristics. Acta Sedimentol. Sin. 28 (5), 926–932 (In Chinese with English abstract).
Gerbersdorf, S.U., Jancke, T., Westrich, B., 2005. Physico-chemical and biological sediment properties determining erosion resistance of contaminated riverine sediments-temporal and vertical pattern at the Lauffen reservoir/River Neckar, Germany. Limnologica 35 (3), 132–144.
Gilbert, G.K., 1914. The transportation of debris by running water. US Gov. Print. Off. 86, 263.
Gordon, C.M., 1974. Intermittent momentum transport in a geophysical boundary layer. Nature 248, 392–394.
Grabowski, R.C., Droppo, I.G., Wharton, G., 2011. Erodibility of cohesive sediment: the importance of sediment properties. Earth Sci. Rev. 105 (3–4), 101–120.
Graf, W.H., 1984. Cohesive-material channels. In: Hydraulics of Sediment Transport. McGraw-Hill, New York, pp. 323–355.
Grass, A.J., 1970. Initial instability of fine bed sand. J. Hydraul. Div. 96 (3), 619–632.
Grass, A.J., 1971. Structural features of turbulent flow over smooth and rough boundaries. J. Fluid Mech. 50 (2), 233–255.
Heathershaw, A.D., 1974. “Bursting” phenomena in the sea. Nature 248, 394–395.
Heathershaw, A.D., Thorne, P.D., 1985. Sea-bed noises reveal role of turbulent bursting phenomenon in sediment transport by tidal currents. Nature 316, 339–342.
Helland-Hansen, E., 1971. Time as a parameter in the study of incipient motion of gravel. In: Annual Meeting of the Northwest Regional Section. American Geophysical Union, Corvallis, Oregon.
Hjulström, F., 1935. Studies of the morphological activity of rivers as illustrated by the River Fyris. Bull. Geol. Inst. 25, 221–527.
Hjulström, F., 1939. Transportation of debris by moving water. In: Trask, P.D. (Ed.), Recent Marine Sediments. A Symposium: Tulsa, Oklahoma, American Association of Petroleum Geologists, pp. 5–31 (Tulsa, Oklahoma).
Inman, D.L., 1949. Sorting of sediments in the light of fluid mechanics. J. Sediment. Petrol. 19, 51–70.
Jacobs, W., Hir, P.L., Kesteren, W.V., Cann, P., 2011. Erosion threshold of sand–mud mixtures. Cont. Shelf Res. 31 (10), S14–S25.
Ji, C., Munjiza, A., Avital, E., Ma, J., Williams, J.J.R., 2013. Direct numerical simulation of sediment entrainment in turbulent channel flow. Phys. Fluids 25 (5), 531–560.
Jiang, J.C., 2019. Theoretical Model for Shields Diagram and its Application. M.S. Thesis. University of Nebraska-Lincoln, pp. 44pp.
Kaller, M.D., Hartman, K.J., 2004. Evidence of a threshold level of fine sediment accumulation for altering benthic macroinvertebrate communities. Hydrobiologia 518 (1), 95–104.
Kassem, H., Thompson, C.E.L., Amos, C.L., Townend, I.H., 2015. Wave-induced coherent turbulence structures and sediment resuspension in the nearshore of a prototype-scale sandy barrier beach. Cont. Shelf Res. 109, 78–94.
Keylock, C.J., 2007. The visualization of turbulence data using a wavelet-based method. Earth Surf. Process. Landforms 32 (4), 637–647.
Kim, S.C., Friedrichs, C.T., Maa, P.Y., Wright, L.D., 2000. Estimating bottom stress in tidal boundary layer from acoustic Doppler velocimeter data. J. Hydraul. Eng. 126 (6), 399–406.
Kline, S.J., Reynolds, W.C., Schraub, F.A., Runstadler, P.W., 1967. The structure of turbulent boundary layers. J. Fluid Mech. 30 (4), 741–773.
Komar, P.D., Li, Z.L., 1986. Pivoting analyses of the selective entrainment of sediments by shape and size with application to gravel threshold. Sedimentology 33 (3), 425–436.
Komar, P.D., Clemens, K.E., 1986. The relationship between a grain's settling velocity and threshold of motion under unidirectional currents. J. Sediment. Petrol. 6 (2), 258–266.
Kramer, H., 1935. Sand mixtures and sand movements in fluvial models. Proc. Am. Soc. Civ. Eng. 100, 798–838.
Kularatne, S., Pattiaratchi, C., 2008. Turbulent kinetic energy and sediment resuspension due to wave groups. Cont. Shelf Res. 28 (6), 726–736.
Lane, E.W., 1955. Design of stable channels. Trans. Am. Soc. Civ. Eng. 120, 413–423.
Lick, W., Jin, L.J., Gailani, J., 2004. Initiation of movement of quartz particles. J. Hydraul. Eng. 755–761.
Ling, C.H., 1995. Criteria for incipient motion of spherical sediment particles. J. Hydraul. Eng. 121 (6), 472–478.
Liu, H.K., 1957. Mechanics of sediment-ripple formation. J. Hydraul. Div. 83 (2), 1–23.
Liu, H.K., 1958. Closure: mechanics of sediment-ripple formation. J. Hydraul. Div. 84 (5), 5–31.
Lu, Y.Z., Wu, J.X., Liu, H., 2012. An integrated post-processing technique for turbulent flows in estuarine bottom boundary layer. Acta Oceanol. Sin. 34 (5), 39–49 (in Chinese with English abstract).
Madsen, O.S., Grant, W.D., 1976. Sediment Transport in the Coastal Environment. Unpublished Technical Report 204. R.M. Parson Laboratory, M.I.T, Cambridge.
Malarkey, J., Baas, J.H., Hope, J.A., Aspden, R.J., Parsons, D.R., Peakall, J., Paterson, M., Schindler, R.J., Ye, L.P., Lichtman, I.D., Bass, S.J., Davies, A.G., Manning, A.J., Thorne, P.D., 2015. The pervasive role of biological cohesion in bedform development. Nat. Commun. 6, 6257. https://doi.org/10.1038/ncomms7257.
Mantz, P.A., 1973. Cohesionless, fine graded, flaked sediment transport by water. Nat. Phys. Sci. (Lond.) 246, 14–16.
Mantz, P.A., 1977. Incipient transport of fine grains and flakes by fluids-extended Shields diagram. J. Hydraul. Div. 103, 601–615.
Mathis, R., Marusic, I., Cabrit, O., Jones, N.L., Ivey, G.N., 2014. Modeling bed shear-stress fluctuations in a shallow tidal channel. J. Geophys. Res. Oceans 119 (5), 3185–3199.
Mathis, R., Marusic, I., Chernyshenko, S.I., Hutchins, N., 2013. Estimating wall-shear-stress fluctuations given an outer region input. J. Fluid Mech. 715, 163–180.
McCave, I.N., 1976. The Benthic Boundary Layer. Plenum press.
Mehta, A.J., 1988. Laboratory Studies on Cohesive Sediment Deposition and Erosion. Physical Processes in Estuaries. Springer-Verlag, pp. 427–445.
Mehta, A.J., Hayter, E.J., Parker, W.R., Krone, R.B., Teeter, A.M., 1989. Cohesive sediment transport. I: process description. J. Hydraul. Eng. 115 (8), 1076–1093.
Mehta, A.J., Lee, S.C., 1994. Problems in linking the threshold condition for the transport of cohesionless and cohesive sediment grain. J. Coast. Res. 10 (1), 170–177.
Mehta, A.J., Partheniades, E., 1979. Kaolinite resuspension properties. J. Hydraul. Div. 105 (4), 409–416.
Mehta, A.J., 2013. An Introduction to Hydraulics of Fine Sediment Transport. World Scientific Publishing Co Pte Ltd.
Miedema, S.A., 2010. Constructing the Shields Curve, a New Theoretical Approach and its Applications. WODCON XIX, Beijing, China, pp. 1–19.
Miedema, S.A., 2013. Constructing the shields curve, Part C: cohesion by silt, hjulstrom, Sundborg. In: Proceedings of the ASME 2013, 32nd International Conference on Ocean, Offshore and Arctic Engineering, Nantes, France, pp. 1–19.
Miller, M.C., McCave, I.N., Komar, P.D., 1977. Threshold of sediment motion under unidirectional currents. Sedimentology 24 (4), 507–527.
Mitchener, H., Torfs, H., 1996. Erosion of mud/sand mixtures. Coast. Eng. 29 (1–2), 1–25.
Morris, W.J., 1957. Effects of sphericity, roundness, and velocity on traction transportation of sand grains. J. Sediment. Res. 27 (1), 27–31.
Nakagawa, H., Nezu, I., 1977. Prediction of the contributions to the Reynolds stress from bursting events in open-channel flows. J. Fluid Mech. 80 (1), 99–128.
Neill, C.R., Yalin, M.S., 1969. Quantitative definition of beginning of bed movement. J. Hydraul. Div. 95 (1), 585–588.
Nelson, J.M., Shreve, R.L., Mclean, S.R., Drake, T.G., 1995. Role of near-bed turbulence structure in bed load transport and bed form mechanics. Water Resour. Res. 31 (8), 2071–2086.
Nishimura, T., 2018. Interaction between moderate earthquakes and volcanic eruptions: analyses of global data catalog. Geophys. Res. Lett. https://doi.org/10.1029/2018GL079060.
Nychas, S.G., Hershey, H.C., Brodkey, R.S., 1973. A visual study of turbulent shear flow. J. Fluid Mech. 61 (3), 513–540.
O'Callaghan, J.M., Pattiaratchi, C.B., Hamilton, D.P., 2010. The role of intratidal oscillations in sediment resuspension in a diurnal, partially mixed estuary. J. Geophys. Res. Oceans 115 (C7), C07018.
Otsubo, K., Muraoka, K., 1988. Critical shear stress of cohesive bottom sediments. J. Hydraul. Eng. 114 (10), 1241–1256.
Paintal, A.S., 1971. Concept of critical shear stress in loose boundary open channels. J. Hydraul. Res. 9 (1), 91–113.
Panagiotopoulos, I., Voulgaris, G., Collins, M.B., 1997. The influence of clay on the threshold of movement of fine sandy beds. Coast. Eng. 32 (1), 19–43.
Paphitis, D., 2001. Sediment movement under unidirectional flows: an assessment of empirical threshold curves. Coast. Eng. 43 (1), 227–245.
Paphitis, D., Collins, M.B., Nash, L.A., Wallbridge, S., 2002. Settling velocities and entrainment thresholds of biogenic sands (shell fragments) under unidirectional flow. Sedimentology 49 (1), 211–225.
Paphitis, D., Velegrakis, A.F., Collins, M.B., Muirhead, A., 2001. Laboratory investigations into the threshold of movement of natural sand-sized sediments under unidirectional, oscillatory and combined flows. Sedimentology 48 (3), 645–659.
Parker, G., Klingeman, P.C., 1982. On why gravel bed streams are paved. Water Resour. Res. 18, 1409–1423.
Paterson, D.M., 1997. Biological mediation of sediment erodibility: ecology and physical dynamics. In: Burt, N., Parker, R., Watts, J. (Eds.), Cohesive Sediments. Wiley Interscience, Chichester, pp. 215–229.
Postma, H., 1967. Sediment transport and sedimentation in the estuarine environment. Am. Assoc. Adv. Sci. 83, 158–179.
Righetti, M., Lucarelli, C., 2007. May the Shields theory be extended to cohesive and adhesive benthic sediments? J. Geophys. Res. Oceans 112 (C5), 395–412.
Roux, J.P.L., 1998. Entrainment threshold of natural grains in liquids determined empirically from dimensionless settling velocities and other measures of grain size.

Sediment. Geol. 119 (1–2), 17–23.
Salehi, M., Strom, K., 2012. Measurement of critical shear stress for mud mixtures in the San Jacinto estuary under different wave and current combinations. Cont. Shelf Res. 47, 78–92.
Salim, S., Pattiaratchi, C., Tinoco, R., Coco, G., Hetzel, Y., Wijeratne, S., Jayaratne, R., 2017. The influence of turbulent bursting on sediment resuspension under unidirectional currents. Earth Surf. Dynam. 5 (3), 1–17.
Salim, S., Pattiaratchi, C., Tinoco, R.O., Jayaratne, R., 2018. Sediment resuspension due to near-bed turbulent effects: a deep sea case study on the northwest continental slope of western Australia. J. Geophys. Res.: Oceans 123 (10), 7102–7119.
Salmond, J.A., 2005. Wavelet analysis of intermittent turbulence in a very stable nocturnal boundary layer: implications for the vertical mixing of ozone. Boundary-Layer Meteorol. 114 (3), 463–488.
Sanford, L.P., Maa, P.Y., 2001. A unified erosion formulation for fine sediments. Mar. Geol. 179 (1–2), 9–23.
Schmeeckle, M.W., Nelson, J.M., 2003. Direct numerical simulation of bedload transport using a local, dynamic boundary condition. Sedimentology 50 (2), 279–301.
Sellar, B., Harding, S., Richmond, M., 2015. High-resolution velocimetry in energetic tidal currents using a convergent-beam acoustic Doppler profiler. Meas. Sci. Technol. 26 (8), 085801.
Shi, B.W., Cooper, J.R., Pratolongo, P.D., Gao, S., Bouma, T.J., Li, G.C., Li, C.Y., Yang, S.L., Wang, Y.P., 2017. Erosion and accretion on a mudflat: the importance of very shallow-water effects. J. Geophys. Res.: Oceans. https://doi.org/10.1002/2016JC012316.
Shi, B.W., Wang, Y.P., Yang, Y., Li, M., Li, P., Ni, W., Gao, J.H., 2015. Determination of critical shear stresses for erosion and deposition based on *in situ* measurements of currents and waves over an intertidal mudflat. J. Coast. Res. 31 (6), 1344–1356.
Shi, Z., Zhou, H.J., 2004. Controls on effective settling velocities of mud flocs in the Changjiang estuary, China. Hydrol. Process. 18 (15), 2877–2892.
Shields, A., 1936. Application of similarity principles and turbulence research to bed-load movement. In: Ott, W.P., Van Uchelen, J.C. (Eds.), Calif. Inst. Of Technol., Pasadena.
Soulsby, R.L., Atkins, R., Salkield, A.P., 1994. Observations of the turbulent structure of a suspension of sand in a tidal current. Cont. Shelf Res. 14 (94), 429–435.
Soulsby, R., 1997. Dynamics of Marine Sands: a Manual for Practical Applications. Thomas Telford.
Sternberg, R.W., Creager, J.S., 1965. An instrument system to measure boundary-layer conditions at the sea floor. Mar. Geol. 3 (6), 475–482.
Sternberg, R.W., 1971. Measurements of incipient motion of sediment particles in the marine environment. Mar. Geol. 10 (2), 113–119.
Sternberg, R.W., 1972. Predicting initial motion and bedload transport of sediment particles in the shallow marine environment. In: Swift, D.J.P., Duane, D.B., Pilkey, O.H. (Eds.), Shelf Sediment Transport. Dowden, Hutchinson and Ross, Stroudsburg, PA, pp. 61–82.
Sundborg, A., 1956. The River Klarälven: a study of fluvial processes. Geogr. Ann. 38, 127–316.
Taki, K., 2001. Critical shear stress for cohesive sediment transport. In: McAnally, W.H., Mehta, A.J. (Eds.), Coastal and Estuarine Fine Sediment Processes. Elsevier Science, Amsterdam, pp. 53–61.
Thomson, R.E., Gordon, R.L., Dymond, J., 1989. Acoustic Doppler current profiler observations of a mid-ocean ridge hydrothermal plume. J. Geophys. Res. Oceans 94 (C4), 4709–4720.
Thorne, P.D., Williams, J.J., Heathershaw, A.D., 1989. *In situ* acoustic measurements of marine gravel threshold and transport. Sedimentology 36 (1), 61–74.
Thorne, P.D., Hardcastle, P.J., Soulsby, R.L., 1993. Analysis of acoustic measurements of suspended sediment. J. Geophys. Res. 98 (98), 899–910.
Tolhurst, T.J., Black, K.S., Shayler, S.A., Mather, S., Black, I., Baker, K., Paterson, D.M., 1999. Measuring the in situ, erosion shear stress of intertidal sediments with the cohesive strength meter (CSM). Estuar. Coast Shelf Sci. 49 (2), 281–294.
Tolhurst, T.J., Consalvey, M., Paterson, D.M., 2008. Changes in cohesive sediment properties associated with the growth of a diatom biofilm. Hydrobiologia 596, 225–239.
Tolhurst, T.J., Jesus, B., Brotas, V., Paterson, D.M., 2003. Diatom migration and sediment armouring - an example from the Tagus Estuary, Portugal. Hydrobiologia 503 (1–3), 183–193.
U.S. Waterways Experimental Station USWES, 1935. Study of River-Bed Material and Their Use with Special Reference to the Lower Mississippi River. Vicksburg MS, pp. 17.
Van Leussen, 1999. The variability of settling velocities of suspended fine-grained sediment in the ems estuary. J. Sea Res. 41 (1–2), 109–118.
Van Rijn, L.C., 1993. Principles of Sediment Transport in Rivers, Estuaries and Coastal Seas. Aqua Publications, Amsterdam.
Vanoni, V.A., 1964. Measurements of Critical Shear Stress for Entraining Fine Sediments in a Boundary Layer. California Institute of Technology.
Vollmer, S., Kleinhans, M.G., 2007. Predicting incipient motion, including the effect of turbulent pressure fluctuations in the bed. Water Resour. Res. 43 (5), 297–304.
Wang, Y.P., Voulgaris, G., Li, Y., Yang, Y., Gao, J., Chen, J., Gao, S., 2013. Sediment resuspension, flocculation, and settling in a macrotidal estuary. J. Geophys. Res. Oceans 118 (10), 5591–5608.
Wilcock, P.R., 1988. Methods for estimating the critical shear stress of individual fractions in mixed-size sediment. Water Resour. Res. 24 (7), 1127–1135.
Willmarth, W.W., Lu, S.S., 1972. Structure of the Reynolds stress near the wall. J. Fluid Mech. 55 (1), 65–92.
Winterwerp, J.C., 2002. On the flocculation and settling velocity of estuarine mud. Cont. Shelf Res. 22 (9), 1339–1360.
Winterwerp, J.C., van Kesteren, W.G.M., 2004. Introduction to the Physics of Cohesive Sediment in the Marine Environment. Elsevier, Amsterdam, pp. 576pp.
Wu, F.C., Lin, Y.C., 2002. Pickup probability of sediment under log-normal velocity distribution. J. Hydraul. Eng. 128 (4), 438–442.
Wu, F.C., Jiang, M.R., 2007. Numerical investigation of the role of turbulent bursting in sediment entrainment. J. Hydraul. Eng. 133 (3), 329–334.
Wu, F.C., Yang, K.H., 2004. Entrainment probabilities of mixed-size sediment incorporating near-bed coherent flow structures. J. Hydraul. Eng. 130 (12), 1187–1197.
Xiong, J.L., Wang, X.H., Wang, Y.P., Chen, J.D., Shi, B.W., Gao, J.H., Yang, Y., Yu, Qian, Li, M.L., Yang, L., Gong, X.L., 2017. Mechanisms of maintaining high suspended sediment concentration over tide-dominated offshore shoals in the southern yellow sea. Estuar. Coast Shelf Sci. 191, 221–233.
Yalin, M.S., 1972. Mechanics of Sediment Transport. Pergamon Press, New York.
Yalin, M.S., Karahan, E., 1979. Inception of sediment transport. J. Hydraul. Div. 105 (11), 1433–1443.
Yang, C.T., 1973. Incipient motion and sediment transport. J. Hydraul. Div. 99 (10), 1679–1704.
Yang, Y., Wang, Y.P., Gao, S., Wang, X.H., Shi, B.W., Zhou, L., Wang, D.D., Dai, C., Li, G.C., 2016a. Sediment resuspension in tidally dominated coastal environments: new insights into the threshold for initial movement. Ocean Dyn. 66 (3), 1–17.
Yang, Y., Wang, Y.P., Li, C.Y., Gao, S., Shi, B.W., Zhou, L., Wang, D.D., Li, G.C., Dai, C., 2016b. On the variability of near-bed floc size due to complex interactions between turbulence, SSC, settling velocity, effective density and the fractal dimension of flocs. Geo Mar. Lett. 36 (2), 135–149.
Yuan, Y., Wei, H., Zhao, L., Cao, Y., 2009. Implications of intermittent turbulent bursts for sediment resuspension in a coastal bottom boundary layer: a field study in the western Yellow Sea, China. Mar. Geol. 263 (1), 87–96.
Zanke, U.C., 1982. Grundlagen der Sedimentbewegung. Springer Verlag, Berlin, Heidelberg, New York.
Zanke, U.C., 2003. On the influence of turbulence on the initiation of sediment motion. Int. J. Sediment Res. 18 (1), 17–31.
Zhang, Q., Gong, Z., Zhang, C., Townend, I., Jin, C., Li, H., 2016. Velocity and sediment surge: what do we see at times of very shallow water on intertidal mudflats? Cont. Shelf Res. 113, 10–20.